Experimental Demonstration of a Temperature-Sensitive VO_2 Memristor-based Spiking Circuit in Stochastic Bursting Regime

Léopold Van Brandt, Noémie Bidoul, Thomas Ratier, Xi Zeng, Jean-Charles Delvenne and Denis Flandre
ICTEAM Institute, UCLouvain, Louvain-la-Neuve, Belgium
leopold.vanbrandt@uclouvain.be

2026 IEEE 17th Latin America Symposium on Circuits and System (LASCAS) | 979-8-3315-7097-2/26/$31.00 ©2026 IEEE | DOI: 10.1109/LASCAS67804.2026.11457126

***Abstract*—Most recent implementations of sensitive neurons based on resistive-switching materials operate in a always-spiking regime, i.e. as relaxation oscillators whose frequency encodes the stimulus. Envisioning future low-energy event-based neuromorphic sensors, we have implemented a temperature-sensitive neuron with a memristor made of vanadium dioxide (VO_2), a phase-change material, capable of exhibiting a stochastic bursting behaviour when biased in subthreshold regime by a MOS transistor. We experimentally demonstrate this functionality by recording intermittent bursts of spikes separated by quiescent periods of time, a behaviour reminiscent of excitable systems. Distinct bursts are unambiguously identified through a rigorous interquartile range method. Temperature is encoded into the temporal characteristics, i.e. the full statistical distribution of these bursts thanks to the temperature dependence of VO_2 transition parameters. The bursts duration and number of spikes per burst are experimentally found to follow an exponential distribution, in agreement with the general theory of Markovian bistable systems. The observed phenomenon could be explained by a noise-induced transient escape from a stable equilibrium to a limit cycle.**

***Index Terms*—Neuromorphic sensor, sensitive spiking neuron, vanadium dioxide, bursting, volatile memristor**

I. Introduction

Phase-change materials such as NbOx and VO_2 exhibit reversible metal-insulator transitions (MIT), i.e. transitions from/to high-resistive state (HRS) to/from low-resistive state (LRS) [1]. Used as volatile memristors, they are able to generate stimulus-dependent electrical spikes [2]–[7], mimicking the action potentials of biological neurons [8]. Prospective applications include neuromorphic sensors, integrated in hardware platforms performing energy-efficient data processing, and neuro-prosthetics devices to restore certain sensory functions among impaired patients [9]. Sensitive neurones have recently been implemented based on two-terminal memristive devices, either by interfacing them with external sensors [10]–[15], or by performing the transduction directly within the phase-change material [7], [16]–[18]. VO_2 is naturally sensitive to various types of stimuli, including temperature [7], strain [19], [20] and light [17], which makes it a promising candidate for neuromorphic multimodal sensors.

This research was supported by the European Research Council (ERC) under the European Union's Horizon AG research and innovation program (ERC-Synergy, SWIMS, 101119062) and the Research Projects "Thermodynamics of Circuits for Computation" and "Stochastic Modelling of Present and Future Nonlinear Dynamical Electronic Devices and Circuits" of the F.R.S.-FNRS.

979-8-3315-7097-2/26/$31.00 ©2026 IEEE

Whereas some biological neurons typically exhibit quiescent periods in between spike events, present sensory neurons either remain silent or operates in always-spiking mode. The latter is also referred to as oscillating regime as the spiking neuron behaves like a relaxation oscillator [17]. In this configuration, the stimulus (e.g. temperature) is encoded in the spike duration or, equivalently, the spike frequency [7]. Such rate-encoding scheme has several flaws in terms of biological plausibility, energy efficiency and robustness against uncertainties.

Firstly, such artificial neurons only mimic the class-1 excitability among the 20 most prominent features of biological neurons [21]. In particular, *excitable* behaviours [22] that would be required to achieve a fully event-based neuromorphic sensing and processing platform [23] are missing. Secondly, the energy consumption of a always-spiking neuron is substantial because of the dynamic consumption inherent to the perpetual charge-discharge process of output capacitors. While the static consumption is usually reported to be dominant and remain to be reduced in future sensor designs [7], [16]–[18], improving the dynamic consumption by using a sparser encoding scheme will be beneficial. Furthermore, sparsity is even more crucial for a hardware configuration where the sensing layer would be interfaced with a spiking neural network [24]. Last but not least, recognised experiments in the field of neuroscience have evidenced that the excitable (i.e. event-based) neuronal behaviours are more robust than the always-spiking ones [25]. The spike timing of the former is precisely determined by the exciting stimulus and is little affected by the unknown noise sources (e.g. generated within the neuron itself), whilst the latter accumulates timing uncertainties across spike cycles [7], i.e. phase errors or *jitter* as is inherent to noisy oscillators [26].

In this work, we present experimental measurements of a temperature-sensitive neuron-like spiking circuit based on a VO_2 memristor operating in *stochastic bursting* regime for the first time to our best knowledge. The transduction is ensured by the variations of the device static current (I) - voltage (V) characteristics with the temperature. We analyse the subsequent spike and burst distributions and statistics. While the reported phenomena still awaits further mathematical modelling, moreover supported by characterisation of the intrinsic noise of the VO_2 memristor, our preliminary analyses suggest that the bursting behaviour could be explained by a noise-induced transient escape from a stable equilibrium to a limit cycle.

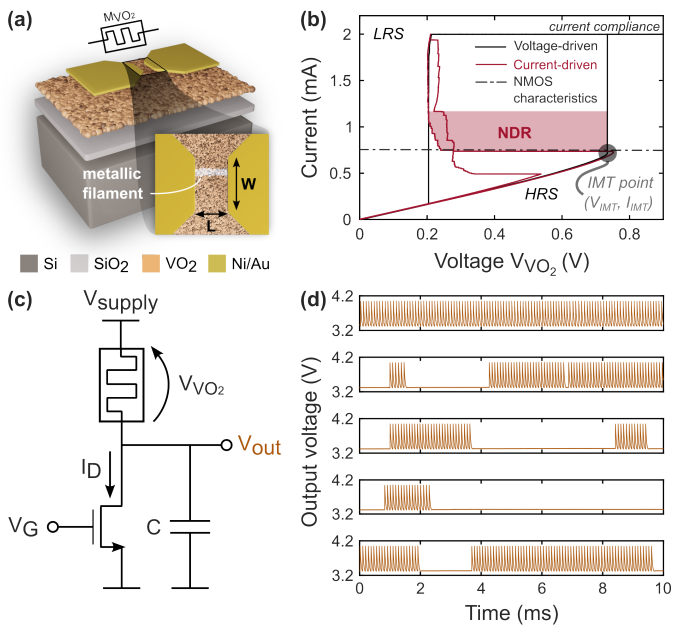

Figure 1. **(a)** Structure of a typical two-terminal VO_2 memristor. **(b)** Static I-V characteristic of the VO_2 device studied in this work ($L = 600\,\mathrm{nm}$ and $W = 3\,\mu\mathrm{m}$), measured in voltage-driven and current-driven modes at $T = 42\,^\circ\mathrm{C}$. The NDR region is shaded in red. The MOS transistor, whose load line at $V_G = 2.04\,\mathrm{V}$ is plotted in dashed line, can be assimilated to a current source setting the operating point. **(c)** Schematics of the VO_2 spiking circuit. **(d)** Five 10 ms-long traces, sampled at 12.5 MHz, showing the bursting output voltage of the circuit.
Parameters: $T = 42\,^\circ\mathrm{C}$, $C = 33\,\mathrm{nF}$, $V_G = 2.04\,\mathrm{V}$ and $V_{supply} = 4.5\,\mathrm{V}$.

II. Experimental Details

The VO_2 memristor, the building block of the spiking neuron, is fabricated on a silicon wafer with a thermally grown 200 nm-thick SiO_2 insulating layer, on which the VO_2 135 nm-thin film is direct-current (DC) sputtered from a vanadium target and further annealed at $500\,^\circ\mathrm{C}$ to trigger crystallization. Since the VO_2 is here not patterned, the device dimensions are defined by the gold electrode dimensions, which are patterned through liftoff. Device structure is shown in Fig. 1(a), with detailed fabrication processes available in [27].

The static I-V characteristics of the device are shown in Fig. 1(b), measured both in voltage- and current-driven modes. The device transitions from its HRS to LRS in a hysteretic fashion. In the current-driven mode, the device shows a negative differential resistance (NDR) across a certain current range, which is a prerequisite to obtain a stable and self-sustained spiking behaviour [28]. NDR takes place in certain devices based on materials whose conductivity has a superlinear temperature dependence [29]. In resistive-switching devices, the transition takes place through a filamentary process, meaning only a portion of the channel becomes metallic. The NDR corresponds to a redistribution of the current flow between the metallic filament and the insulating outer part in the channel.

The schematics of the spiking circuit implemented on PCB is depicted in Fig. 1(c), following [7]. In this work, only the VO_2 memristor is placed on the heating chunk and is subject to controlled temperature variations. Output voltage traces (like those shown in Figure 1(d)) are recorded with an oscilloscope.

III. Spiking Circuit Operation

To drive the VO_2 memristor into continuous oscillations (i.e. spiking regime), a bias current must be applied in its NDR, without intersecting other stable points in its I-V curve, placing the device in an unstable configuration. The current is here controlled by the gate voltage of a series NMOS transistor (see Fig. 1(c)). A capacitor sets the charge and discharge time constants, and hence the spiking rate [7]. The energy consumption is dominated by the static power, in the mW range, which remains to be improved in future implementations.

The spiking circuit of Fig. 1(c) can be regarded as a nonlinear dynamical system with two equilibrium behaviours, depending on the bias current: either a stable equilibrium point, corresponding to a silent neuron, or a limit cycle (in the I-V plan) when the neuron spikes. *Hopf bifurcations* can explain the appearance of a limit cycle in *deterministic* systems, notably the oscillating behaviours of different types of spiking neurons, based on memristors or not [30], [31]: the limit cycle emerges (i.e. the neuron spikes) when a static parameter of the circuit (here the bias current) exceeds a certain critical threshold (here I_{IMT} as indicated in Fig. 1(b)). When setting the transistor drain current I_D at the edge of the NDR region (right above the current level I_{IMT}), oscillations become unstable. The device thus emits bursts of spikes (see measured time series in Fig. 1(d)). Such behaviour has been associated to the phase-locked firing, skipping, or tonic bursting in biological neurons [6].

Regarding the circuit of Fig. 1(c)), random *transient noise* is believed to induce the stochastic transitions from the stable equilibrium to the limit cycle. Akin to stochastic resonance [32], however in absence of periodic forcing signal, bursting phenomena occur when the amplitude and duration of the noise is sufficient to briefly enter the stable oscillation region. The origin of such triggering noise remains to be thoroughly investigated. It is likely intrinsic to the spiking neuron circuit of Figure 1(c), i.e. it includes all the noise sources of the VO_2 memristor and of the MOS transistor. Previous work [7] suggested that the intrinsic stochasticity of the memristor was dominated by time-uncorrelated cycle-to-cycle variations of the hysteresis parameters. However, this hypothesis requires further validation by experiments and modelling.

IV. Temperature-Dependent Stochastic Bursting

The temperature-dependence of the VO_2 device I-V curve, captured by the Poole-Frenkel conduction mechanism [18], [33], allows to encode temperature into the bursts temporal characteristics. Such dependence is shown experimentally in Fig. 2(a), with current-driven measurements performed in the 41 to $47\,^\circ\mathrm{C}$ temperature range (corresponding to a noxious temperature range for humans [34]). As the VO_2 conductivity increases rapidly with temperature, the Joule power required to bring a portion of the VO_2 channel to insulator-to-metal transition and induce filament formation reduces, progressively lowers the corresponding IMT bias point with respect to the fixed NMOS current (see Fig. 2(b)). The resulting bursting

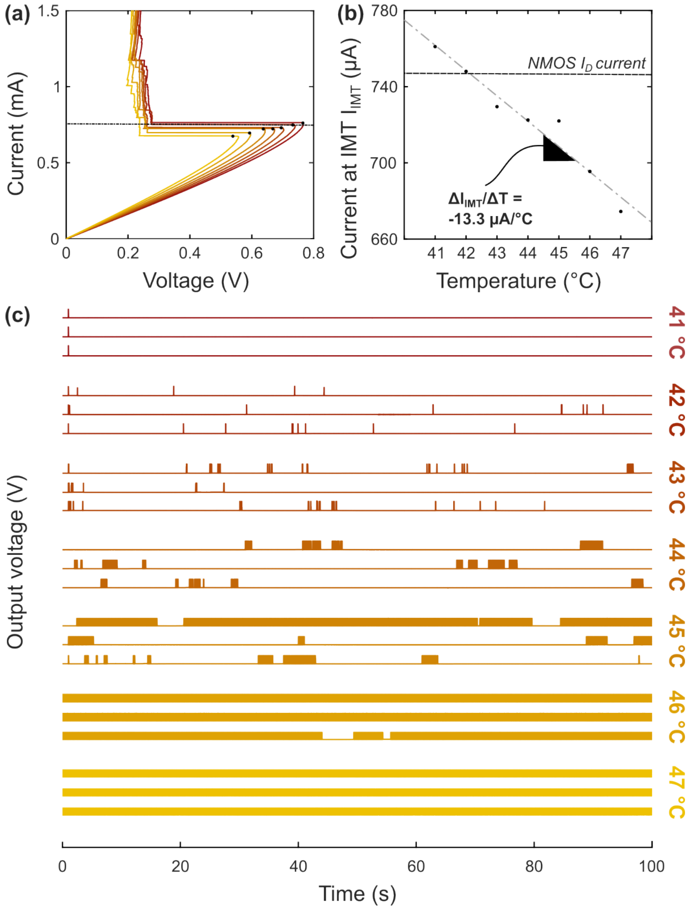

Figure 2. **(a)** Evolution of the VO_2 device current-driven I-V characteristics with temperature, in the 41 °C (red) - 47 °C (yellow) temperature range. Only the forward-part of the hysteresis is shown. **(b)** Extraction of the current level I_{IMT} corresponding to the IMT, plotted against temperature. **(c)** For each temperature point, three 100 s-long traces of the circuit output voltage were sampled at 100 kHz.

behaviour has been recorded through three 100 s-long measurements at each temperature (Fig. 2(c)).

For the device to exhibit stable and sustained oscillations, the biasing current must be a least tens of μA *larger* than the IMT current I_{IMT} (as it is the case at 47 °C): this can be regarded as a noise margin ensuring a certain immunity to the established stable limit cycle. At lower temperatures, e.g. 41 to 43 °C, the biasing current falls *below* I_{IMT} and bursts occur very sparsely. This occurs because the memristor is there set in a stable equilibrium point at the end of the hysteresis branch corresponding to the insulating state (near the $(V_{\mathrm{IMT}}, I_{\mathrm{IMT}})$ point of Fig. 2(b)): as temperature increases, the system escapes more easily from the basin of attraction of the stable equilibrium point due to the noise, i.e. the probability of observing a burst increases. In the intermediate temperature range, bursts duration tends to increase with temperature. This phenomenon is attributed to a degradation of the noise immunity of the stable equilibrium point that lies at the verge of instability as the temperature rises. Past observations of bursts in resistive-switching neurons were modulated by varying the amplitude of the current fed through the device [35], [36], or by artificially adding a certain amount of noise to this current [6], [32], [37].

In this work, since the control current is fixed, the temperature-dependent I-V characteristics progressively bring the system towards fully spiking regime, resulting in the observed stimuli-dependent bursting behaviour for the intermediate temperature range.

V. Statistical Analyses and Discussion

To study the stochastic bursting phenomenon, we focus on the 42 - 45 °C temperature range where bursts are not too sparse nor too frequent. The goal is to understand which specific burst metrics encode the stimulus. These metrics are defined in Fig. 3(a)-(b), including the burst duration T_b, the number of spikes per burst N_s and the inter-spike interval *ISI*. These quantities are random and require statistical analyses. The firing rate is defined as the total number of spikes fired over the entire observation time, in spike/s. Even in the field of neurosciences, there is no clear consensus on unambiguous quantitative definitions of "spikes" and "bursts" [8]. Therefore, an important methodological question is to define when two consecutive spikes should be considered as part of the same burst or distinct bursts. In this work, separate bursts are identified through the Interquartile Range (IQR) method, as depicted in Fig. 3(c)-(f). The IQR, or "box-plot" method, is commonly used to detect outliers within a dataset [38]. For each temperature, all ISIs are extracted over a full observation duration, and the three quartiles $Q1$, $Q2$ and $Q3$ dividing the ISIs dataset into four equal intervals (each containing 25 % of the data) are computed. Two consecutive spikes whose ISI is larger than the threshold $ISI_{th} = Q3 + 1.5 \cdot IQR$ are considered to belong to distinct bursts.

Based on this definition, Fig. 3(g)-(h) show that the bursts duration and the number of spikes per burst follow an exponential distribution (shown here at 43 °C, but observed for all four temperatures). Importantly, the exponential distribution is entirely characterized by its mean λ, which is also equal to its standard deviation. Fig. 3(j) and (k) show that the means of the two parameters (burst duration, number of spikes per burst) increase exponentially with temperature. The mean ISI within a burst (Fig. 3(i)) decreases linearly with temperature (consistently with past observations in always-spiking sensitive neurons [7], [12], [18]), while the firing rate (Fig. 3(l)) increases exponentially with temperature. Interestingly, evolutions of the burst parameters with temperature (shown in Fig. 3(i)-(l)) follow similar trends than those measured in sensory neurons of certain insects in reaction to noxious heat [39], [40], which might be an asset regarding the biophysical plausibility of the reported bursting behaviour.

Regarding the stochasticity of the bursting phenomenon, the exponential distribution of the bursts duration and number of spikes per burst has been observed previously in FitzHugh–Nagumo oscillators [41], analog neuromorphic circuits exemplifying excitable systems [22]. The exponential distribution is a rather general property of *transition times* in Markovian bistable systems with time-scale separation [42], [43] an instance of which are CMOS memory bitcells prone to state variation caused by the intrinsic noise [44]. This analogy has led us to presumably attribute the experimentally reported

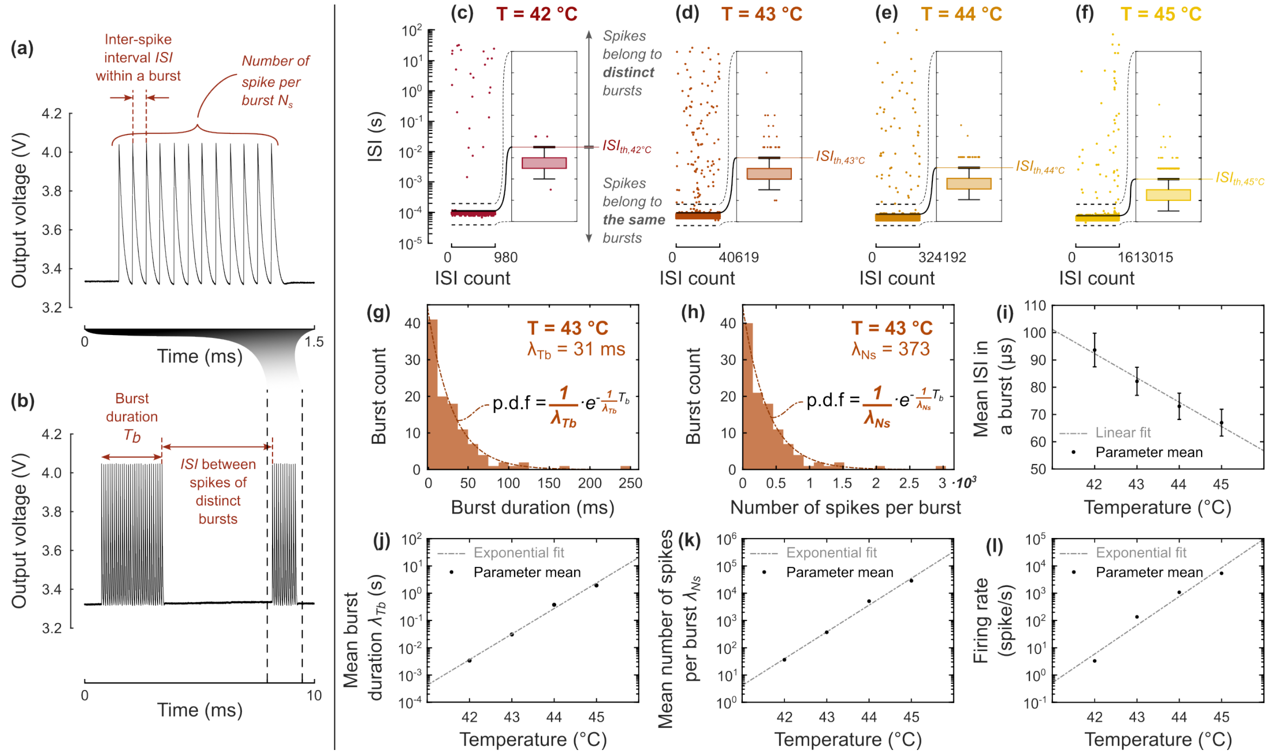

Figure 3. Evolution of the bursts characteristics between 42 and 45 °C. **(a)(b)** Definition of the different bursts metrics. **(c)-(f)** Statistical definition of a burst. For each temperature, the dataset of ISIs extracted for each pair of consecutive spikes is shown together with the dataset box-plot. The upper boundary corresponds to the ISI threshold for burst definition: pairs of consecutive spikes whose ISI is below ISI_{th} belong to the same burst. Distribution of the bursts duration **(g)** and number of spikes per burst **(h)** measured at 43 °C, fitted to an exponential distribution. Evolution of several burst metrics with temperature : mean ISI in a burst **(i)**, mean burst duration **(j)**, mean number of spikes per burst **(k)** and firing rate **(l)**.

bursting phenomena to noise-induced transient escape from the basin of attraction of a stable equilibrium point to a limit cycle. This interpretation is consistent with the numerical simulation of [41]. Notably, an increase of the temperature seems to increase the probability of such transitions and therefore the burst and spike densities (Fig. 3(c)-(f)).

Our conjecture could be strengthened and validated by future mathematical modelling work driven by experimental VO_2 device data. Such approach would combine concepts from nonlinear systems theory applied to memristor-based neurons [31] with stochastic calculus [43].

VI. Conclusion & Perspectives

We have here experimentally reported a stimulus-dependent stochastic bursting behaviour in a simple one VO_2 memristor - one transistor circuit, with transduction of the temperature directly performed within the VO_2 device. Distinct bursts have been unambiguously identified through a rigorous interquartile range method. Stimulus information is contained both in the statistics of the burst and in the firing rate, unlike recent implementations of VO_2 memristor-based sensors that operate in rate-encoding, i.e. always-spiking mode. While the experimental distributions suggest that the stochastic bursting phenomenon is attributed to a noise-induced state transition from a stable equilibrium to a limit cycle, further modelling work are still required to confirm this assumption. Moreover, the reproducibility of the reported behaviour across multiple devices should be assessed in future work. The static energy consumption remains to be improved to fully benefit from such sparser encoding scheme. Future neuromorphic sensors could leverage the natural sensitivity of VO_2 to other types of stimuli such as strain and light. This paves the way for a new generation of energy-efficient and bio-plausible sensitive spiking neurons.

References

[1] R. Carboni and D. Ielmini, "Stochastic memory devices for security and computing," *Advanced Electronic Materials*, vol. 5, no. 9, p. 1900198, 2019.

[2] M. D. Pickett, G. Medeiros-Ribeiro, and R. S. Williams, "A scalable neuristor built with Mott memristors," *Nature Materials*, vol. 12, no. 2, pp. 114–117, dec 2013, DOI: https://doi.org/10.1038/nmat3510.

[3] R. Yuan, P. J. Tiw, L. Cai, Z. Yang, C. Liu, T. Zhang, C. Ge, R. Huang, and Y. Yang, "A neuromorphic physiological signal processing system based on VO2 memristor for next-generation human-machine interface," *Nature Communications*, vol. 14, no. 1, p. 3695, jun 2023, DOI: https://doi.org/10.1038/s41467-023-39430-4.

[4] A. Parihar, M. Jerry, S. Datta, and A. Raychowdhury, "Stochastic IMT (Insulator-Metal-Transition) Neurons: An Interplay of Thermal and Threshold Noise at Bifurcation," *Frontiers in Neuroscience*, vol. 12, p. 210, apr 2018, DOI: https://doi.org/10.3389/fnins.2018.00210.

[5] S. M. Bohaichuk, S. Kumar, G. Pitner, C. J. McClellan, J. Jeong, M. G. Samant, H.-S. P. Wong, S. S. P. Parkin, R. S. Williams, and E. Pop, "Fast Spiking of a Mott VO2–Carbon Nanotube Composite Device," *Nano Letters*, aug 2019, DOI: https://doi.org/10.1021/acs.nanolett.9b01554.

[6] W. Yi, K. K. Tsang, S. K. Lam, X. Bai, J. A. Crowell, and E. A. Flores, "Biological plausibility and stochasticity in scalable VO2 active memristor neurons," *Nature Communications*, vol. 9, no. 1, p. 4661, nov 2018, DOI: https://doi.org/10.1038/s41467-018-07052-w.

[7] N. Bidoul, T. Rosca, A. M. Ionescu, and D. Flandre, "Static and Dynamic Stochastic Analysis of a Temperature-Sensitive VO $_2$ Spiking Neuron,"

in *ESSDERC 2023 - IEEE 53rd European Solid-State Device Research Conference (ESSDERC)*, oct 2023, pp. 81–84.
[8] C. Koch, *Biophysics of computation: information processing in single neurons*. Oxford university press, 2004.
[9] Y. Wu, Y. Liu, Y. Zhou, Q. Man, C. Hu, W. Asghar, F. Li, Z. Yu, J. Shang, G. Liu, M. Liao, and R.-W. Li, "A skin-inspired tactile sensor for smart prosthetics," *Science Robotics*, vol. 3, no. 22, p. eaat0429, sep 2018, DOI: https://doi.org/10.1126/scirobotics.aat0429.
[10] F. Li, R. Wang, C. Song, M. Zhao, H. Ren, S. Wang, K. Liang, D. Li, X. Ma, B. Zhu, H. Wang, and Y. Hao, "A Skin-Inspired Artificial Mechanoreceptor for Tactile Enhancement and Integration," *ACS Nano*, vol. 15, no. 10, pp. 16 422–16 431, oct 2021, DOI: https://doi.org/10.1021/acsnano.1c05836.
[11] S. L. Fang, C. Y. Han, W. Liu, Z. R. Han, B. Ma, Y. L. Cui, S. Q. Fan, X. Li, X. L. Wang, G. H. Zhang, J. Q. Yin, X. D. Huang, and L. Geng, "A bioinspired flexible artificial mechanoreceptor based on VO2 insulator-metal transition memristor," *Journal of Alloys and Compounds*, vol. 911, p. 165096, aug 2022, DOI: https://doi.org/10.1016/j.jallcom.2022.165096.
[12] R. Yuan, Q. Duan, P. J. Tiw, G. Li, Z. Xiao, Z. Jing, K. Yang, C. Liu, C. Ge, R. Huang, and Y. Yang, "A calibratable sensory neuron based on epitaxial VO2 for spike-based neuromorphic multisensory system," *Nature Communications*, vol. 13, no. 1, p. 3973, jul 2022, DOI: https://doi.org/10.1038/s41467-022-31747-w.
[13] J. Zhu, X. Zhang, R. Wang, M. Wang, P. Chen, L. Cheng, Z. Wu, Y. Wang, Q. Liu, and M. Liu, "A Heterogeneously Integrated Spiking Neuron Array for Multimode-Fused Perception and Object Classification," *Advanced Materials*, vol. 34, no. 24, p. 2200481, apr 2022, DOI: https://doi.org/10.1002/adma.202200481.
[14] X. Zhang, Y. Zhuo, Q. Luo, Z. Wu, R. Midya, Z. Wang, W. Song, R. Wang, N. K. Upadhyay, Y. Fang, F. Kiani, M. Rao, Y. Yang, Q. Xia, Q. Liu, M. Liu, and J. J. Yang, "An artificial spiking afferent nerve based on Mott memristors for neurorobotics," *Nature Communications*, vol. 11, no. 1, p. 51, jan 2020, DOI: https://doi.org/10.1038/s41467-019-13827-6.
[15] Q. Wu, B. Dang, C. Lu, G. Xu, G. Yang, J. Wang, X. Chuai, N. Lu, D. Geng, H. Wang, and L. Li, "Spike Encoding with Optic Sensory Neurons Enable a Pulse Coupled Neural Network for Ultraviolet Image Segmentation," *Nano Letters*, vol. 20, no. 11, pp. 8015–8023, Nov. 2020, DOI: https://doi.org/10.1021/acs.nanolett.0c02892.
[16] F. Qaderi, T. Rosca, M. Burla, J. Leuthold, D. Flandre, and A. M. Ionescu, "Millimeter-wave to near-terahertz sensors based on reversible insulator-to-metal transition in VO2," *Communications Materials*, vol. 4, no. 1, pp. 1–12, may 2023, DOI: https://doi.org/10.1038/s43246-023-00350-x.
[17] T. Rosca, F. Qaderi, and A. M. Ionescu, "High Tuning Range Spiking 1R-1T VO2 Voltage-Controlled Oscillator for Integrated RF and Optical Sensing," in *ESSCIRC 2021 - IEEE 47th European Solid State Circuits Conference (ESSCIRC)*, oct 2021, pp. 183–186, DOI: https://doi.org/10.1109/ESSCIRC53450.2021.9567761.
[18] C. Y. Han, Z. R. Han, S. L. Fang, S. Q. Fan, J. Q. Yin, W. H. Liu, X. Li, S. Q. Yang, G. H. Zhang, X. L. Wang, and L. Geng, "Characterization and Modelling of Flexible VO2 Mott Memristor for the Artificial Spiking Warm Receptor," *Advanced Materials Interfaces*, vol. 9, no. 19, p. 2200394, jun 2022, DOI: https://doi.org/10.1002/admi.202200394.
[19] J. Cao, E. Ertekin, V. Srinivasan, W. Fan, S. Huang, H. Zheng, J. W. L. Yim, D. R. Khanal, D. F. Ogletree, J. C. Grossman, and J. Wu, "Strain engineering and one-dimensional organization of metal–insulator domains in single-crystal vanadium dioxide beams," *Nature Nanotechnology*, vol. 4, no. 11, pp. 732–737, sep 2009, DOI: https://doi.org/10.1038/nnano.2009.266.
[20] Z. S. Somaehsofla, C. Masserey, A. Varini, D. Flandre, and A. M. Ionescu, "Wafer-scale demonstration of a highly sensitive strain sensor based on polycrystalline VO2," in *2025 IEEE 38th International Conference on Micro Electro Mechanical Systems (MEMS)*. IEEE, 2025, pp. 635–638.
[21] E. Izhikevich, "Which Model to Use for Cortical Spiking Neurons?" *IEEE Transactions on Neural Networks*, vol. 15, no. 5, pp. 1063–1070, sep 2004, DOI: https://doi.org/10.1109/TNN.2004.832719.
[22] R. Sepulchre, G. Drion, and A. Franci, "Excitable behaviors," in *Emerging Applications of Control and Systems Theory: A Festschrift in Honor of Mathukumalli Vidyasagar*. Springer, 2018, pp. 269–280.
[23] S.-C. Liu, T. Delbruck, G. Indiveri, A. Whatley, and R. Douglas, *Event-based neuromorphic systems*. John Wiley & Sons, 2014.
[24] C. Frenkel, "Sparsity provides a competitive advantage," *Nature Machine Intelligence*, vol. 3, no. 9, pp. 742–743, sep 2021, DOI: https://doi.org/10.1038/s42256-021-00387-y.
[25] Z. F. Mainen and T. J. Sejnowski, "Reliability of spike timing in neocortical neurons," *Science*, vol. 268, no. 5216, pp. 1503–1506, 1995.
[26] M. Bonnin, "Amplitude and phase dynamics of noisy oscillators," *International Journal of Circuit Theory and Applications*, vol. 45, no. 5, pp. 636–659, 2017.
[27] N. Bidoul, N. Roisin, and D. Flandre, "Tuning the Intrinsic Stochasticity of Resistive Switching in VO2 Microresistors," *Nano Letters*, may 2024, DOI: https://doi.org/10.1021/acs.nanolett.4c00184.
[28] G. A. Gibson, "Designing Negative Differential Resistance Devices Based on Self-Heating," *Advanced Functional Materials*, vol. 28, no. 22, p. 1704175, apr 2018, DOI: https://doi.org/10.1002/adfm.201704175.
[29] S. K. Nandi, S. K. Nath, A. E. El-Helou, S. Li, X. Liu, P. E. Raad, and R. G. Elliman, "Current Localization and Redistribution as the Basis of Discontinuous Current Controlled Negative Differential Resistance in NbOx," *Advanced Functional Materials*, vol. 29, no. 50, p. 1906731, oct 2019, DOI: https://doi.org/10.1002/adfm.201906731.
[30] E. M. Izhikevich, "Neural excitability, spiking and bursting," *International journal of bifurcation and chaos*, vol. 10, no. 06, pp. 1171–1266, 2000.
[31] A. Ascoli, A. S. Demirkol, I. Messaris, V. Ntinas, D. Prousalis, S. Slesazeck, T. Mikolajick, F. Corinto, M. Bonnin *et al.*, "Edge of chaos theory unveils the first and simplest ever reported hodgkin–huxley neuristor," *Advanced Electronic Materials*, vol. 11, no. 8, p. 2400789, 2025.
[32] B. Bhar, A. Khanna, A. Parihar, S. Datta, and A. Raychowdhury, "Stochastic Resonance in Insulator-Metal-Transition Systems," *Scientific Reports*, vol. 10, no. 1, p. 5549, mar 2020, DOI: https://doi.org/10.1038/s41598-020-62537-3.
[33] G. A. Gibson, S. Musunuru, J. Zhang, K. Vandenberghe, J. Lee, C.-C. Hsieh, W. Jackson, Y. Jeon, D. Henze, Z. Li, and R. Stanley Williams, "An accurate locally active memristor model for S-type negative differential resistance in NbOx," *Applied Physics Letters*, vol. 108, no. 2, p. 023505, jan 2016, DOI: https://doi.org/10.1063/1.4939913.
[34] N. A. Martin and S. Falder, "A review of the evidence for threshold of burn injury," *Burns: Journal of the International Society for Burn Injuries*, vol. 43, no. 8, pp. 1624–1639, dec 2017, DOI: https://doi.org/10.1016/j.burns.2017.04.003.
[35] M. Jerry, A. Parihar, B. Grisafe, A. Raychowdhury, and S. Datta, "Ultra-low power probabilistic IMT neurons for stochastic sampling machines," in *2017 Symposium on VLSI Technology*, aug 2017, pp. T186–T187, DOI: https://doi.org/10.23919/VLSIT.2017.7998148.
[36] H. Liu, X. Zhu, Z. Guo, R. He, X. Li, Q. Sun, X. Ye, C. Sun, Y. Tian, and R.-W. Li, "Artificial Spiking Neuron with Bursting Dynamics for Noise-Resistant Neuromorphic Coding," *ACS Applied Electronic Materials*, vol. 5, no. 6, pp. 3454–3461, jun 2023, DOI: https://doi.org/10.1021/acsaelm.3c00445.
[37] M. Drouhin, S. Li, M. Grelier, S. Collin, F. Godel, R. G. Elliman, B. Dlubak, J. Trastoy, D. Querlioz, and J. Grollier, "Characterization and modeling of spiking and bursting in experimental NbO_x neuron," *Neuromorphic Computing and Engineering*, vol. 2, no. 4, p. 044008, oct 2022, DOI: https://doi.org/10.1088/2634-4386/ac969a.
[38] J. W. Tukey, *Exploratory data analysis*, ser. Addison-Wesley series in behavioral sciences. Reading, Mass.: Addison-Wesley Pub. Co., 1977, DOI: https://doi.org/10.1007/978-0-387-32833-1_136.
[39] E. Merivee, A. Must, K. Nurme, A. Di Giulio, M. Muzzi, I. Williams, and M. Mänd, "Neural Code for Ambient Heat Detection in Elaterid Beetles," *Frontiers in Behavioral Neuroscience*, vol. 14, feb 2020, DOI: https://doi.org/10.3389/fnbeh.2020.00001.
[40] A. Must, E. Merivee, K. Nurme, I. Sibul, M. Muzzi, A. D. Giulio, and I. Williams, "Encoding noxious heat by spike bursts of antennal bimodal hygroreceptor (dry) neurons in the carabid Pterostichus oblongopunctatus," *Cell and Tissue Research*, vol. 368, no. 1, pp. 29–47, dec 2017, DOI: https://doi.org/10.1007/s00441-016-2547-y.
[41] N. Albanbay, B. Medetov, and M. A. Zaks, "Exponential distribution of lifetimes for transient bursting states in coupled noisy excitable systems," *Chaos: An Interdisciplinary Journal of Nonlinear Science*, vol. 31, no. 9, p. 093105, sep 2021, DOI: https://doi.org/10.1063/5.0059102.
[42] J. Rinzel, "A formal classification of bursting mechanisms in excitable systems," in *Mathematical Topics in Population Biology, Morphogenesis and Neurosciences: Proceedings of an International Symposium held in Kyoto, November 10–15, 1985*. Springer, 1987, pp. 267–281.
[43] L. Van Brandt and J.-C. Delvenne, "Predicting State Transitions in Autonomous Nonlinear Bistable Systems with Hidden Stochasticity," *IEEE Control Systems Letters*, 2024.
[44] L. Van Brandt, M. Bonnin, M. B. da Silva, P. Bolcato, G. I. Wirth, D. Flandre, and J.-C. Delvenne, "Modeling and Predicting Noise-Induced Failure Rates in Ultra-Low-Voltage SRAM Bitcells Affected by Process Variations," *IEEE Transactions on Circuits and Systems I: Regular Papers*, 2025.